PHYSICAL REVIEW C VOLUME 21, NUMBER 6 JUNE 1980

# Proton-nucleus charge exchange measurements at 144 MeV as a test of one-pion exchange and the partially conserved axial vector current

G. L. Moake,* L. J. Gutay, and R. P. Scharenberg
*Department of Physics, Purdue University, West Lafayette, Indiana 47907*

P. T. Debevec†
*Department of Physics, Indiana University, Bloomington, Indiana 47405*

P. A. Quin
*Department of Physics, University of Wisconsin, Madison, Wisconsin 53706*
(Received 29 October 1979)

We have measured the differential cross sections of the $(p,n)$ reaction on $^6$Li, $^{12}$C, and $^{14}$N to the ground state of the final nucleus ($\Delta J = 1$, $\Delta T = 1$, $\Delta\pi = 0$) and to the 7.77 MeV excited state of $^{14}$O at $E_p = 144$ MeV and $0° < \theta_{lab} < 20°$. For the ground state cases, we treat the nuclei as elementary particles, which are assigned the initial nucleus-pion-final nucleus coupling constants predicted using the partially conserved axial vector current. The Born helicity amplitudes for one-pion exchange are presented along with a method for including distortions in momentum space. The calculations which have no free parameters agree with the data for $^6$Li and $^{12}$C, but not for $^{14}$N.

[NUCLEAR REACTIONS $^6$Li$(p,n)$, $^{12}$C$(p,n)$, and $^{14}$N$(p,n)$ at $E_p = 144$ MeV. Differential cross sections measured between 0° and 20° (lab). Initial nucleus-pion-final nucleus coupling constants extracted.]

## I. INTRODUCTION

In nuclear physics we have become accustomed to the concept of a nucleon-nucleon potential which has its fundamental foundations in the theoretical premise of meson exchange. Our understanding of this potential, while by no means complete, is rather advanced. It is well known, for example, that a realistic potential must contain both central and noncentral components and must be momentum dependent. There cannot be a simple correspondence between components of this potential and individual meson exchanges. However, since the pion is the least massive meson, one-pion exchange must become dominant at large distances. In fact, a comparison of the one-pion exchange potential to a phenomenological force which reproduces the nucleon-nucleon phase shifts, e.g., the Hamada-Johnston potential, shows that one-pion exchange is dominant in the spin-isospin component and the isovector tensor component at distances as small as the Compton wavelength of the pion.[1] Yet at these intermediate ranges, it is necessary to introduce the exchange of scalar mesons, both isoscalar and isovector, which represent the effective contribution of nonresonant two-pion exchange. In order to account for the other components of the central interaction at shorter distances and to characterize the short range repulsion, even the most sophisticated calculations must become phenomenological at small distances. The understanding of the nucleon-nucleon interaction in terms of meson exchange is then largely successful, especially at large distances or equivalently, at high partial waves.

When one considers the scattering of nucleons from a nucleus, the complexity of the many-body problem makes the *ab initio* description of the nuclear force in terms of meson exchange unfeasible. However, the transition of the nucleus from one state of definite spin, parity, and isospin to another imposes definite limitations on the meson exchanges that can occur (assuming a single interaction which may be valid at intermediate energies). For nuclear transitions of $J=0 \nrightarrow J=1$, $T=0 \nrightarrow T=1$, and $\pi=1 \nleftrightarrow \pi=1$, the meson exchange must transfer one unit of angular momentum and isospin without changing the parity. Thus, for interactions of medium and long range, which correspond to scattering in the forward direction, the reaction may be dominated by one-pion exchange. One-pion exchange is known to contribute to $n+p \rightarrow p+n$ charge exchange scattering where the quantum number restrictions are not so severe. There, one-pion exchange manifests itself in a large forward peak.[2] This peak is not reflected in most nuclear inelastic scatterings, however, but the quantum numbers of most transitions are inconsistent with one-pion exchange. For the transitions with quantum numbers listed above, we

 

may expect one-pion exchange in the forward direction, producing a forward peak. In order to test this hypothesis, we have measured the forward angle cross sections for the $(p,n)$ reaction on $^{6}$Li, $^{12}$C, and $^{14}$N to the resulting ground states; these transitions all have $\Delta J=1$, $\Delta T=1$, $\Delta\pi=0$.

If the reaction at forward angles is dominated by one-pion exchange, then one has an opportunity to test the application of the partially conserved axial vector current hypothesis (PCAC) to nuclei in a novel way, as first suggested by Kim and Primakoff.[3] The proposal is to consider the initial and final nuclear states as elementary particles, specifying only the mass, spin, parity, and isospin, and to introduce a vertex function which characterizes the coupling of the initial nucleus, a pion, and the final nucleus. By application of PCAC, one can derive a relation similar to the Goldberger-Treiman relation,[4] which relates the initial nucleus-pion-final nucleus coupling for a virtual pion to the matrix element of the axial vector current $\langle N'|A_\alpha(x)|N\rangle$. This matrix element is known from the $\beta$ decay of the final nucleus $N'$ to the initial nucleus $N$. In a similar manner, PCAC can be used to relate the momentum transfer dependence of the vertex function $g_{N\pi N'}(q^2)$ to that of an inelastic electron scattering form factor. Since the axial vector matrix elements for the cases considered herein are known (assuming $^{6}$Be$\rightarrow{}^{6}$Li has the same matrix element as $^{6}$He$\rightarrow{}^{6}$Li), and since the required inelastic electron scattering form factors have been measured, then in principle the one-pion exchange differential cross section for $p+N\rightarrow n+N'$ can be calculated.

It is useful to make a comparison between this proposal and the more conventional procedure. Present day nuclear inelastic scattering calculations in the intermediate energy range are typically made with an effective interaction in the distorted wave impulse approximation (DWIA).[5,6] The effective interaction is chosen to have (on-shell) matrix elements which reproduce the nucleon-nucleon scattering amplitudes in the intermediate energy range. The functional form of the interaction is usually taken to be a sum of Yukawa functions $e^{-\mu r}/\mu r$; a slightly different functional form is used for the tensor force. Generally there is one term in the effective interaction with the range and strength appropriate for one-pion exchange, with other terms representing interactions of shorter range. The interaction is folded over the entire nucleus using nuclear wave functions, which reflect the structure of the states involved, to produce an inelastic scattering form factor. In certain cases the transition density measured in inelastic electron scattering can be used directly. The scattering waves in the initial and final states are generated from an optical potential which reproduces the measured elastic scattering. The transition amplitude then is the integral of the inelastic scattering form factor and the two distorted waves. Although this method incorporates one-pion exchange, the exchange is only between individual nucleons, and there is no means of introducing the initial nucleus-pion-final nucleus vertex function. Thus, it is not possible to test the application of the PCAC hypothesis to nuclei.

We have chosen to use the one-particle exchange model developed for particle physics applications[7-9] known as the absorption model to incorporate initial and final state distortions. Since the Born amplitudes for meson exchange are most naturally expressed in momentum space, the absorption model modifies the Born amplitudes to account for initial and final state distortions in momentum space. Since at high energy the elastic scattering potential is primarily absorptive, the inclusion of distortions merely reduces the magnitude of each partial wave of the Born amplitudes. Hence, the method is known as the absorption model.

Our calculational procedure, then, was to begin with the Born helicity amplitudes for one-pion exchange represented by the Feynman diagram shown in Fig. 1. The proton-pion-neutron vertex is known from pion-nucleon scattering, and the initial nucleus-pion-final nucleus vertex function at zero momentum transfer $g_{N\pi N'}(0)$ was obtained from PCAC. The dependence of the two vertices on momentum transfer was obtained from PCAC using in the nuclear case the inelastic electron scattering form factor. Thus, the Born amplitudes

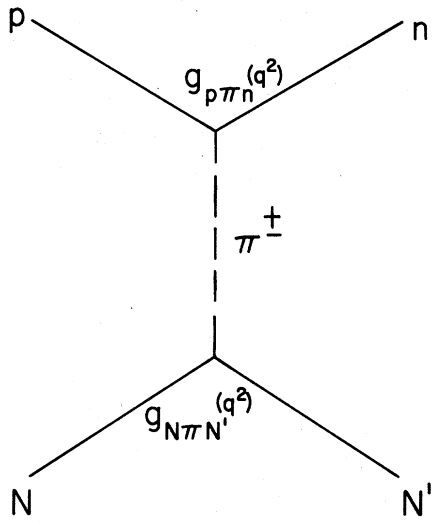


FIG. 1. One-pion exchange diagram for the reaction $p+N\rightarrow n+N'$ in the Born approximation.

were completely determined. Initial and final state interactions were inserted through the absorption model, although changes in the model were made to make it more applicable to scattering from a nucleus. Neglected in our calculations are explicit two-step processes and exchange terms arising from antisymmetrization between the projectile and the target nucleons. Multistep processes, however, are probably well accounted for by use of an optical potential which reproduces elastic scattering.[10] The exchange term may be neglected for forward scattering at intermediate energy for these transitions of low multipolarity. It is easy to see in impulse approximation that the exchange term is proportional to $v(|\vec{k}+\vec{k}'|)$, which is much smaller than the direct term which is proportional to $v(|\vec{k}-\vec{k}'|)$.[11] It is also the case that we neglect all contributions from other meson exchanges (or equivalently, other components of the effective interaction which would contribute upon antisymmetrization). Again, for transitions of low multipolarity and for forward scattering this neglect should not be serious. One-pion exchange does include the tensor component.

As our calculations are performed in momentum space, they appear radically different from the traditional nuclear physics calculations. In fact, they are actually quite similar to the effective interaction calculations of Petrovich,[12] which are also formulated in momentum space. Petrovich argues that the momentum space calculations are useful as they can make direct use of information obtained on the momentum components of the transition density from inelastic electron scattering. (The argument is persuasive even though electron scattering does not provide all of the transition densities required for nucleon scattering.) When the traditional calculation is written in momentum space, the parallel to our calculation becomes clear. Our Born amplitudes with the nuclear vertex function removed corresponds to the effective interaction, and our nuclear vertex function corresponds to the transition density. The distortions due to initial and final state interactions are inserted in each method. The difference between the two methods is simply that the traditional calculation performs an integral over momentum to account for the spatial extent of the nucleus, while we approximate the integration by choosing a mean value. It is shown below that our approximation should be adequate; it does in fact produce a very similar reduction in the differential cross section compared to the Born amplitudes, as does the distorted wave impulse approximation when compared to the plane wave impulse approximation.[13]

It should be noted that our application of PCAC to nuclei is rather different than its usual application to elementary particles. There, the differences between the coupling to nucleons of virtual pions and real pions can be ignored. We make no statement from our analysis, from which we obtain $g_{N\pi N'}(0)$, on the coupling of the nucleus to real pions, $g_{N\pi N'}(-m_\pi^2)$. This question has been raised in other applications of PCAC to nuclei, namely, muon capture,[14,15] radiative pion capture,[14,16] and pion scattering.[17] In our application we assume that PCAC is exact, or rather the Goldberger-Treiman relation (as stated) is exact, and compare our calculation to the measured differential cross sections. Our proposal also differs from the original suggestion of Kim and Primakoff,[3] who suggested an extrapolation of the measured $(p,n)$ differential cross section into the unphysical region, the pion pole. This procedure has its difficulties even in application to nucleon charge exchange. Similarly, extraction of one-pion exchange from the higher partial waves of the $(p,n)$ differential cross section would be extremely difficult. At the very least, a rather complete angular distribution would be required for a partial wave analysis; and although the forward scattering appears to have a large component from one-pion exchange, many other processes may contribute to the scattering at larger momentum transfers.[18] We find rather good agreement between our assumptions of one-pion exchange and the applicability of PCAC and our measured differential cross sections. Although this agreement does not uniquely justify our assumptions, it does give them a certain amount of credence.

## II. EXPERIMENTAL PROCEDURE AND RESULTS

### A. Apparatus

The experiment was carried out at the Indiana University Cyclotron Facilty (IUCF). The experimental area is shown in Fig. 2. The target assembly was placed inside the chamber and just before the pole faces. Steel cylinders were placed inside and outside of the entrance beam pipe to prevent the beam from being bent in the magnetic field before it hit the target. The main proton beam was swept by the magnetic field into a Faraday cup buried in the wall, whereas the forward scattering neutrons emerged from the chamber through a 0.076 mm thick kapton window. Neutrons destined to reach the detector had to pass through very restrictive collimation, as shown in Fig. 3. The vertical collimation was supplied by stacked lead and concrete blocks, and the horizontal collimation was provided by lead bricks stacked on carts. This allowed the detector to view only the target. The scattering angle was changed by moving the detector, which was placed on a mobile hut. Angles

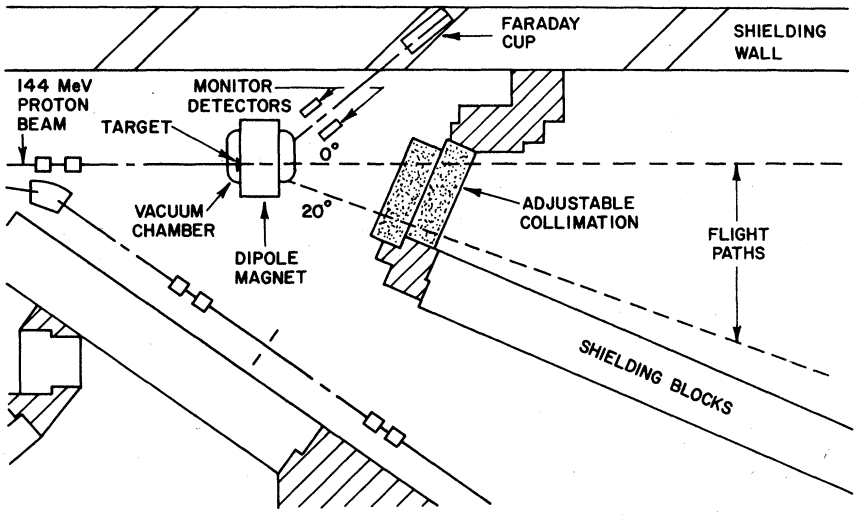


FIG. 2. Floor plan of the experimental area.

from 4° beam left to 25° beam right could be obtained and flight paths of 20 and 25 m were employed. A beam energy of 144 MeV was chosen because it was one of the maximum energies available at IUCF at that time and because good elastic scattering data for the $^{6}$Li and $^{12}$C existed at that energy.[19]

The detector used is shown in Fig. 4. It consisted of a sheet of plastic scintillator (charged particle identifier) followed by two NE 102 plastic scintillator timing rods (45.7 cm long and 4.44 cm in diameter), which in turn were followed by a vat of NE 213 liquid scintillator (50.8 cm long, 25.4 cm high, and 15.2 cm deep). The rods and vat were viewed at both ends by phototubes. Timing signals from each end of a rod were used to start a TAC, which was stopped by the subsequent rf pulse. The signals from the two ends of a rod were then added in the computer. Since the rod was thin, the resulting spectrum represented the time between the projectile leaving the target and the time it interacted in the rod. Pulse height signals from both ends of each rod and both ends of the vat were summed individually in hardware and were also stored. Timing signals from the charged particle identifier and the rods were used to produce an analog routing signal, whose magnitude depended on whether the detected particle was charged or not (interacted in the charged particle identifier or not), and on the rod with which it had interacted. In this way, both neutron and proton pulse height and time-of-flight spectra could be observed. (Although the bending magnet turned the main proton beam into the beam dump, it also bent elastically scattered protons toward the detector. The horizontal collimation could usually be arranged to block these particles, but some were always allowed to pass, providing a useful diagnostic tool.) Wrap-around, the contribution to

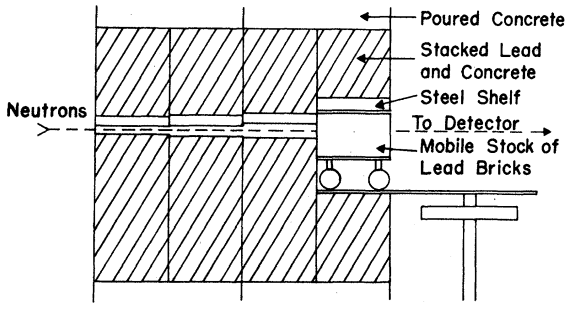


FIG. 3. Schematic drawing of the neutron collimator.

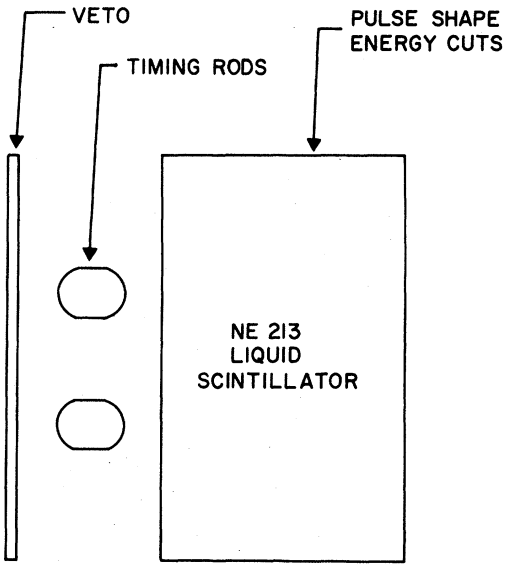


FIG. 4. Drawing of the neutron detector.

the time spectrum originating from neutrons that were so slow that they would reach the detector at the same time as a faster neutron from a later burst, was always eliminated by setting a software threshold on the vat energy. The threshold required to eliminate wrap-around depends on the beam repetition rate (~30 MHz), as well as the flight path. Since the higher the pulse height threshold detection, the lower the efficiency, the beam repetition rate was reduced by pulse selecting one out of four beam bunches (4×32 nsec) before main stage acceleration. Because of low beam currents during the initial phase of the experiment, the $^6$Li data were taken with no pulse selection.

Two monitor counters, a plastic scintillator, and an NaI crystal, were placed outside of the vacuum chamber, downstream from the target, on either side of the exit beam line. Kapton windows in the chamber allowed protons elastically scattered at about 7° to reach these detectors relatively unhindered. The plastic scintillator was used as a monitor of the target thickness, while the NaI crystal was used to monitor the beam arrival time relative to the cyclotron rf phase. Owing to instabilities in the cyclotron, the time at which the beam was extracted relative to a signal generated from an rf crossing would drift. By stopping the protons in the NaI crystal, measuring their time of flight against the rf, and using the energy signal to choose only elastically scattered protons, the beam arrival time fluctuations were measured in an average way by observing the shifts in the flight time of the elastically scattered protons.

The signals that were monitored on-line and stored in event mode were the time of flight of both sides of the rods, the rod energy, the vat energy, the router, and the time of flight from the NaI monitor. The latter was recorded asynchronously to allow off-line corrections for beam arrival time variations.

The targets used were natural carbon and 98.5% enriched $^6$Li; they were about 55 mg/cm$^2$ thick and presented a 300 keV loss to the proton beam. The full energy loss of the proton in the target is reflected in the resolution of the scattered neutrons. A nitrogen target was obtained by using melamine ($N_6C_3H_6$); the $Q$ value for $(p,n)$ on carbon is high enough so that reactions on carbon do not interfere with the $^{14}$O ground state. The melamine target was about 70 mg/cm$^2$ thick, causing a 350 keV loss to the proton beam.

### B. Data reduction

The first step in the data reduction was to correct the time-of-flight spectra for beam arrival time drifts. This correction was done by calculating for each 100 events recorded in the NaI monitor the centroid of their time of flight. This centroid was compared to an arbitrary time reference. The corresponding events in the neutron detector (which occurred in real time over the same period of time as the monitor signal) were then shifted in the opposite direction by the appropriate amount. Depending on the mood of the accelerator, this would give a 6% to 25% reduction in the FWHM.

The pulse height spectrum of the vat was calibrated from the position of the elastically scattered proton peak using the known light output for protons in NE 213. Thus the threshold required to eliminate wrap-around could be determined, and events with vat pulse heights below this threshold were ignored. Using the router signal, the data were then sorted into four time-of-flight arrays, representing protons and neutrons in each rod. Peak areas were then extracted by fitting Gaussian curves on a quadratic background to the data. For the $^6$Li and melamine targets, the resolution was sufficient to easily distinguish the ground state peak from the first excited state. For the carbon target, however, the first excited state was only six-tenths of a FWHM away. Although better resolution is desired, this resolution should give reasonable results. Actually, there was no indication of the first several excited states being present, and chi-squares/degrees of freedom near one were obtained by assuming that they were absent. Statistical errors were calculated by finding the area for which the total chi-square was increased by one. The results from the two rods were then averaged.

Dead time corrections for the computer and TAC's were made. The router pulses were scaled as well as stored by the computer, so that the computer dead time could be obtained. Dead time in only one of the TAC's manifested itself in a poor resolution time spectrum superimposed on the principal one. The ratio of these two was then obtained from the proton spectra to determine the TAC dead time. The total of these corrections was always less than 10%.

The magnetic shielding before the target could not totally prevent the incident beam from bending before hitting the target, so the true beam direction $\theta_0$ had to be determined. Consequently, cross sections for $^6$Li were measured at the nominal angles of 0, ±1, and ±2°. A function quadratic in $|\theta - \theta_0|$ was then fitted to the data, yielding $\theta_0 = -0.3 \pm 0.3°$. Thus, all nominal angles were increased by 0.3°.

### C. Normalization

The detector efficiency and solid angle were calibrated by normalizing the carbon data to

data taken with a liquid scintillator detector measuring 12.7 cm deep and 12.7 cm in diameter. This detector was calibrated for 130 MeV neutrons in an independent experiment,[20] in which a tagged neutron beam was produced using the reaction $p + {}^7\mathrm{Li} \rightarrow n + {}^7\mathrm{Be}$. A small correction for the neutron absorption by air was also made. We estimate that the normalization of all the data, including the efficiency and target thickness, is ±7%; the errors indicated are statistical. Our final differential cross sections for $^6$Li are in excellent agreement with the $(n,p)$ data of Measday and Polmieri obtained at 152 MeV.[21] From charge symmetry the two differential cross sections should be equal.

### D. Results

The forward angle spectra for the three targets are shown in Fig. 5. For the case of mass 6 and 12, the ground state clearly dominates the spectrum, but this is certainly not true for the case of mass 14. Indeed, in this case, the ground state is extremely small, and the spectrum is dominated by the 7.77 MeV $(2^+;1)$ excited state of $^{14}$O. After corrections for the beam arrival time, the time resolution varied from 0.85 to 1.0 nsec. From the proton spectra we inferred that the time resolution was mainly limited by the beam itself. The corresponding energy resolution was between 1.7 and 2.0 MeV.

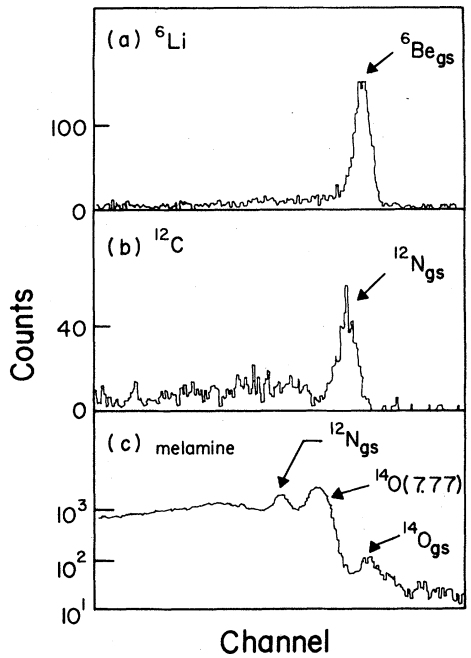


FIG. 5. The 0.3° time-of-flight spectrum for (a) $p + {}^6\mathrm{Li} \rightarrow n + {}^6\mathrm{Be}$, (b) $p + {}^{12}\mathrm{C} \rightarrow n + {}^{12}\mathrm{N}$, and (c) $p$ + melamine $\rightarrow n + X$.

The measured cross sections for the ground states and oxygen excited state are shown in Fig. 6. They are all forward peaked, but the $^{14}$O ground state is much flatter than the others. The excited state of $^{14}$O is almost identical to the mass 12 case, indicating that they may be produced by the same mechanism.

## III. THEORETICAL ANALYSIS

### A. Scattering amplitudes

We first start by writing down the general form of the Born amplitudes corresponding to the Feynman diagram shown in Fig. 1,

$$T^{\kappa}_{\lambda'\lambda} = 2 g_{N\pi N'}(q^2) g_{p\pi n}(q^2) \frac{\bar{u}^{\lambda'}(\vec{p}')\gamma_5 u^{\lambda}(\vec{p})}{q^2 + m_\pi^2} \xi_\nu^{(\kappa)}(\vec{p}') q_\nu . \quad (1)$$

The indices of the helicity amplitude $T^{\kappa}_{\lambda'\lambda}$ denote the helicity of the spin-1 nucleus $\kappa$ and the initial and final nucleon helicities ($\lambda$ and $\lambda'$). The proton-pion-neutron and initial nucleus-pion-final nucleus vertex functions are represented by $g_{p\pi n}(q^2)$ and $g_{N\pi N'}(q^2)$, respectively, and are functions of the four-momentum transfer squared, $q^2$. Also, $u^{\lambda}(\vec{p})$ is the Dirac spinor with helicity $\lambda$ and momentum $\vec{p}$, $\xi_\nu^{(\kappa)}(\vec{p}')$ is the spin-1 function (polarization vector) with helicity $\kappa$ and momentum $\vec{p}'$, $\xi_\nu$ is the four-momentum transfer, and $\gamma_5$ is the usual Dirac operator. There are twelve different amplitudes $T^{\kappa}_{\lambda'\lambda}$, but space reflection can be used to relate six of them to the other six by[7]

$$T^{-\kappa}_{-\lambda'-\lambda} = (-1)^{\kappa+\lambda+\lambda'} T^{\kappa}_{\lambda'\lambda} . \quad (2)$$

A set of six independent amplitudes are written below in a form in which the angular dependence and momentum transfer dependence are explicitly denoted:

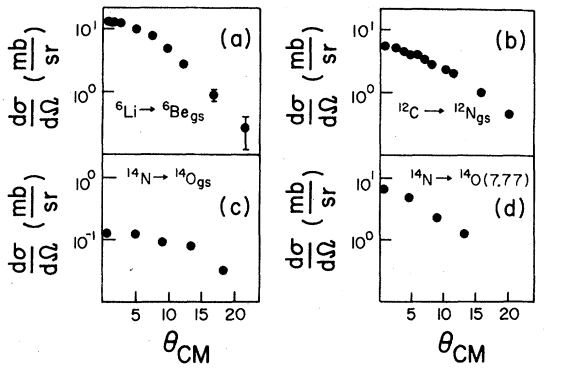


FIG. 6. The differential charge exchange cross section for (a) $p + {}^6\mathrm{Li} \rightarrow n + {}^6\mathrm{Be}$ (ground state), (b) $p + {}^{12}\mathrm{C} \rightarrow n + {}^{12}\mathrm{N}$ (ground state), (c) $p + {}^{14}\mathrm{N} \rightarrow n + {}^{14}\mathrm{O}$ (ground state), and (d) $p + {}^{14}\mathrm{N} \rightarrow n + {}^{14}\mathrm{O}$ (7.77 MeV, $2^+$ state).

$$T^0_{++}=g_{p\pi n}(q^2)g_{N\pi N'}(q^2)b\xi_-\frac{E_1}{M_1}\left\{-d^{1/2}_{1/2,1/2}(\theta)+(z-\gamma)\frac{\cos(\theta/2)}{z-\cos\theta}\right\}, \tag{3a}$$

$$T^0_{+-}=g_{p\pi n}(q^2)g_{N\pi N'}(q^2)b\xi_+\frac{E_1}{M_1}\left\{d_{-1/2,1/2}(\theta)+(z-\gamma)\frac{\sin(\theta/2)}{z-\cos\theta}\right\}, \tag{3b}$$

$$T^1_{++}=g_{p\pi n}(q^2)g_{N\pi N'}(q^2)\frac{b}{\sqrt{2}}\xi_-\left\{-d^{1/2}_{-1/2,1/2}(\theta)+(z+1)\frac{\sin(\theta/2)}{z-\cos\theta}\right\}, \tag{3c}$$

$$T^1_{--}=-g_{p\pi n}(q^2)g_{N\pi N'}(q^2)\sqrt{2}\,b\xi_-\frac{\sin(\theta/2)\cos^2(\theta/2)}{z-\cos\theta}, \tag{3d}$$

$$T^1_{+-}=g_{p\pi n}(q^2)g_{N\pi N'}(q^2)\frac{b}{\sqrt{2}}\xi_+\left\{d^{1/2}_{1/2,1/2}(\theta)-(z-1)\frac{\cos(\theta/2)}{z-\cos\theta}\right\}, \tag{3e}$$

$$T^1_{-+}=g_{p\pi n}(q^2)g_{N\pi N'}(q^2)\sqrt{2}\,b\xi_+\frac{\sin^2(\theta/2)\cos(\theta/2)}{z-\cos\theta}. \tag{3f}$$

Our notation is similar to that of Refs. 7–9, which consider $\pi+p\to p+n$, which has the same spin sequence and is described by one-pion exchange. The angle $\theta$ denotes the center of mass angle of the neutron, and $d^{1/2}_{\lambda'\lambda}(\theta)$ denotes the rotation function of order $\frac{1}{2}$. The rest of the symbols are defined in Table I. These helicity amplitudes then represent the one-pion exchange Born approximation to the $(p,n)$ reaction for $0^+\to 1^+$ transitions.

### B. Extraordinary terms

It is seen from Eqs. (3) that four of the Born amplitudes contain an $s$-wave contribution in the form of $d^{1/2}_{\lambda'\lambda}$. These terms are referred to as the "extraordinary" terms in the literature and must be removed from the Born amplitudes before a comparison can be made to experimental data. The appearance of extraordinary terms is quite general in one-boson exchange Born amplitudes, and they are often removed.[22] There does not appear to be a universal consensus on the justification for this procedure. The fact that these terms are troublesome is easily seen by plotting the contribution to the Born amplitudes of each partial wave, as is done in Fig. 7. Without the extraordinary terms, the amplitudes are seen to be continuous functions of the angular momentum. However, if the extraordinary terms are included, then the $s$-wave ($j=\frac{1}{2}$) amplitudes become negative while all other partial waves are unmodified, causing a

TABLE I. Variables of Eq. (3) not defined in the text.

| Variable | Definition |
|---|---|
| $b$ | $1/p'$ for $J=0\to1$ transitions and $1/p$ for $J=1\to0$ transitions |
| $\chi_\pm$ | $\{(E+m_p)(E'+m_n)\}^{1/2}\{p/(E+m_p)\pm p'/(E'+m_n)\}$ |
| $\xi_\pm$ | $\chi$ for $J=0\to1$ transitions and $-\chi$ for $J=1\to0$ transitions |
| $z$ | $(2EE'+m_\pi{}^2-m_n{}^2-m_p{}^2)/2pp'$ |
| $\gamma$ | $p'E_N/pE_{N'}$ for $J=0\to1$ and $pE_{N'}/p'E_N$ for $J=1\to0$ |
| $E_1$ | Center of mass energy of the nucleus with spin 1 |
| $M_1$ | Mass of the nucleus with spin 1 |
| $m_n$ | Neutron mass |
| $m_p$ | Proton mass |
| $m_\pi$ | Charged pion mass |

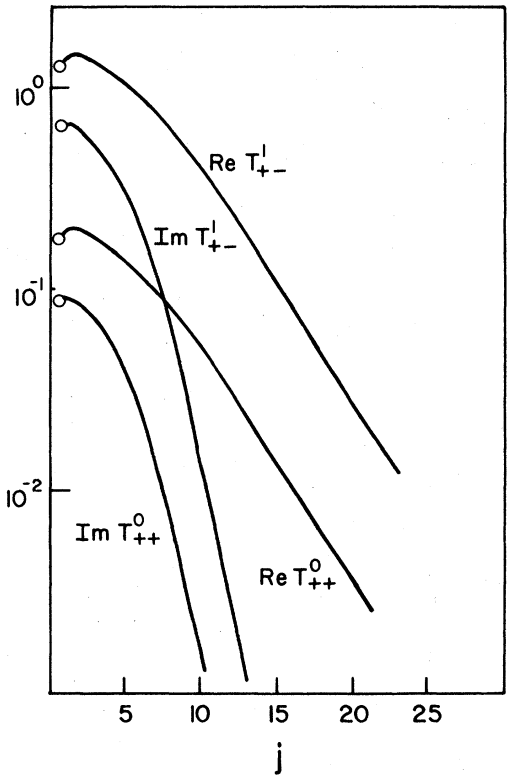


FIG. 7. Plot of the partial waves of the nonzero one-pion exchange amplitudes at 0°, including the distorted wave modification. A curve has been drawn through the discrete half-integer points to guide the eye. If the extraordinary terms were to be included, then the only difference would be that the $j=\frac{1}{2}$ points would become negative.

discontinuity. In the elementary particle literature it is noted that the extraordinary terms will violate $s$-wave unitarity, an absolute constraint, and thus their removal is justified.[8,23] The argument is also formulated with reference to the peripheral (high partial wave) nature of one-particle exchange processes that the Born amplitudes are simply inadequate for the lower partial waves. If one transforms the Born amplitudes to coordinate space, then the extraordinary terms become a $\delta$ function in the relative coordinate. In the one-pion exchange potential, this $\delta$ function is called a "contact" term. As one would expect, this term is traditionally discarded in the coordinate space formulation as well.[24] With respect to the nucleon-nucleon one-boson exchange potential, the argument is put forth that the short range repulsion prevents the contact term from contributing. More complicated arguments also have been formulated.[25] Although it is certainly the case that one-pion exchange cannot be the dominant contribution at small distances, the removal of the contact term has a rather simple justification for the Born approximation. A repulsive $\delta$ function can cause no contribution to the scattering amplitude because the boundary condition on the wave function requires that it vanish identically for $r=0$. Thus, if only Born approximation is considered and not the solution to the Schrödinger equation, it is more correct to neglect the $\delta$ function completely.

It is perhaps worthwhile to digress and to mention the relevance of these considerations for the historical determination of the pion-nucleon coupling constant from nucleon-nucleon scattering. Two rather different methods have been applied. Recognizing that one-pion exchange becomes dominant at large distances, the phase shifts for the high partial waves of intermediate energy scattering ($\lesssim 450$ MeV) should be totally determined by the one-pion exchange potential. Thus, the magnitude of the coupling constant can be fixed by a best fit of the one-pion exchange potential to the $L \gtrsim 4$ partial waves.[26] In this manner the well-known number $g^2/4\pi = 14.6$ is obtained. We have argued that an analogous procedure would probably fail in the nuclear application. The second method follows the observation of Chew that the singularity in the scattering amplitude (the pion pole)[27] lies close to the physical region. The suggestion was made that a rather modest extrapolation of the differential cross section into the unphysical region would provide the pion-nucleon coupling constant. However, the Born amplitude for one-pion exchange in $n+p \to p+n$ vanishes at zero degrees (the effect of the extraordinary or the contact term) and the ubiquitous charge exchange peak in $n+p \to p+n$ was obtained through the interference of the one-pion exchange Born amplitude and smooth background terms. It is surprising then that the extrapolation procedure applied by Ashmore *et al.*[28] could obtain approximately the pion-nucleon coupling constant, a result which may be ascribed to a rather judicious choice of the data set and the order of the extrapolated polynomial. It is seen in the extrapolation performed by Cziffra and Moravcsik[29] that nonsensical results are obtained if the polynomial is either of too low or too high an order. The suggestion has been made that more optimal extrapolation procedures can be employed[30]; we do not feel competent to comment on this suggestion. Instead, we continue with the method described in the Introduction: Having introduced the Born amplitudes, we modified them to account for distortions introduced by the initial and final state interactions, and chose vertex functions consistent with the PCAC hypothesis.

Once the extraordinary term has been removed, it is easy to see which of the amplitudes in Eq. (3) is dominant. Since $\xi_-$ is essentially zero, only $T^0_{+-}$, $T^1_{+-}$, and $T^1_{-+}$ need be considered. These are the amplitudes corresponding to the projectile flipping its helicity. Of them, $T^1_{+-}$ is dominant at forward angles, which is easily seen by examining their angular dependence.

### C. Absorption model

It is not surprising that a method for doing distorted wave calculations in momentum space was developed in elementary particle physics, as almost all of their calculations are done in momentum space. The method was developed because of the discrepancy between one-pion exchange Born approximation calculations and various experiments in which one-pion exchange was firmly believed to dominate the reaction. Historically, in the first attempt to remove this discrepancy, arbitrary vertex functions were introduced. However, in order to fit the data, these phenomenological functions had to be much stronger than was thought reasonable. It was realized that the effect of these form factors was to reduce the contribution of the lower partial waves to the scattering amplitude. Consequently, a more natural way of doing this was sought. With the realization that the existence of scattering channels other than the one being observed would reduce the amplitudes of the lower partial waves and with the concurrent application of distorted wave techniques in nuclear physics, the absorption model was born.[7,8]

The absorption model includes distortions by modifying each partial wave of the Born amplitudes by a factor accounting for the effect of the elastic scattering on that partial wave. A rather simple form can be derived under the assumptions

that (1) the particle wavelengths are small compared to the characteristic ranges of the interactions, (2) the entrance and exit channels are strongly coupled to many inelastic channels, and (3) the range of the exchange interaction is small compared to that of other interactions.[2] It must be admitted that these assumptions are invalid in nuclear physics; they are also of questionable validity in particle applications. The form of the modification in our calculation is

$$T^{\kappa,j}_{\lambda',\lambda} = \tfrac{1}{4}\{(S_i^{j,j+1/2})^{1/2} + (S_i^{j,j-1/2})^{1/2} + (S_f^{j,j+1/2})^{1/2} + (S_f^{j,j-1/2})^{1/2}\} T^{\kappa,j}_{\lambda',\lambda}(\text{Born}) , \tag{4}$$

where $S_i^{j,l}(S_f^{j,l})$ is the elastic scattering $S$ matrix element for the incident (scattered) particle and $T^{\kappa,j}_{\lambda,\lambda}(\text{Born})$ is the $j$th partial wave Born helicity amplitude, which is obtained from $T^{\kappa}_{\lambda',\lambda}(\text{Born})$ by the technique of Hogaasen and Hogassen.[9] The justification of Eq. (4) is given in the Appendix and holds only for forward angles. It will be noted that Eq. (4) differs from that used in elementary particle physics in two ways. One way is that $S$ is taken to depend on the orbital angular momentum $l$ as well as $j$. The primary difference, however, is that $S$ is raised to the one-half power instead of the first power, which accounts for the range of the elastic and inelastic potentials being comparable in a nucleus.

The $S$ matrix elements were calculated from the optical potentials for the target nuclei at 144 MeV,[31] using the optical model code SNOOPY.[32] The potential for the final nucleus was assumed to be that of the target, so the final $S$ matrix elements were calculated for a neutron with the appropriate energy. The sensitivity of the $(p,n)$ cross section to uncertainties in the $S$ matrix elements was estimated for $^{12}$C by calculating it for a potential optimized to the differential cross section and to a potential optimized to polarization data. The results differed by only 5%. The sensitivity could be greater for $^{6}$Li, however, since the potential is not as well determined.

### D. Vertex functions

As pointed out by Kim and Primakoff,[3] the magnitude of an initial nucleus-pion-final nucleus vertex function at zero momentum transfer can be obtained by applying PCAC to the nuclear states to obtain a nuclear Goldberger-Treiman relation. The original Goldberger-Treiman relation[4] was a proportionality between the proton-pion-neutron coupling constant $g_{p\pi n}(-m_\pi^2)$ and the axial vector coupling constant measured in neutron $\beta$ decay $g_A(0)$. The nuclear relation, which we derive below, is a proportionality at $q^2=0$ between the initial nucleus-pion-final nucleus vertex function $g_{N\pi N'}(q^2=0)$ and the weak axial vector coupling constant $F_A(q^2=0)$, for the $N' \to N + e^+ + \nu$ decay. In this approach the nucleus is treated as an elementary particle in the sense that only the spin, parity, isospin, and mass of the nuclear states are explicitly specified. It has also been shown by Kim[33] that the dependence of the nuclear vertex function $g_{N\pi N'}(q^2)$ for transitions dominated by no change of orbital angular momentum can be obtained from the inelastic electron scattering form factor $\mu(q^2)$. Kim also shows that the corrected Goldberger-Treiman relation for nucleons can be used to estimate the dependence on momentum transfer of the pion-nucleon vertex function $g_{p\pi n}(q^2)$. The arguments go as follows.

PCAC, in the formulation of Gell-Mann and Levy,[34] states that

$$\partial_\alpha A_\alpha(x) = a_\pi m_\pi^3 \phi(x) , \tag{5}$$

where $A_\alpha(x)$ is the weak axial vector current, $\phi(x)$ is the pion field operator that creates or destroys a pion, $m_\pi$ is the pion mass, and $a_\pi = 0.939$ is the pion decay constant, determined from $\pi \to \mu + \nu$. If one treats the nucleus as an elementary particle, then $A_\alpha(x)$ can only be constructed from vector quantities pertaining to the nucleus as a whole.

For $0^\pm \to 1^\pm$ transitions, one has

$$\langle N'_\kappa | A_\alpha(x) | N\rangle = 2(M_N M_{N'})^{1/2}\left\{\xi_\alpha^{(\kappa)} F_A(q^2) + q_\alpha \xi_\mu^{(\kappa)} q_\mu \frac{F_P(q^2)}{m_\pi^2} + (P_\alpha^N + P_\alpha^{N'})\xi_\mu^{(\kappa)} q_\mu \frac{F_T(q^2)}{m_\pi^2}\right\} e^{-iq_\nu x_\nu} . \tag{6}$$

The symbols $M_N$ and $M_{N'}$ stand for the masses of the nuclei $N$ and $N'$; $\xi_\alpha^{(\kappa)}$ is the usual spin-1 function with helicity $\kappa$; $F_A(q^2)$, $F_P(q^2)$, and $F_T(q^2)$ are, respectively, the axial vector, induced pseudoscalar, and induced tensor weak nuclear form factors; $P_\alpha^N$ and $P_\alpha^{N'}$ are the momenta of $N$ and $N'$ with the momentum transfer $q_\alpha = P_\alpha^N - P_\alpha^{N'}$; and $x_\nu$ is the position at which the current is evaluated. The matrix element of the pion field, $\langle N'_\kappa | \phi | N\rangle$, can be broken into an expansion of terms represented by the diagrams shown in Fig. 8. Evaluating only the first term in the expansion gives

$$\langle N'_\kappa | \phi | N\rangle = -2i \frac{\xi_\alpha^{(\kappa)} q_\alpha}{q^2 + m_\pi^2} g_{N\pi N'}(q^2) . \tag{7}$$

With the PCAC choice of the pion field, Eqs.

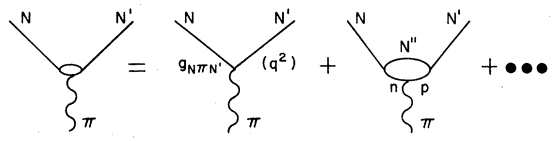


FIG. 8. Diagramatic representation of the two lowest order terms of the pion field matrix element $\langle N' | \phi | N \rangle$ in covariant perturbation theory.

(5)–(7) can be combined to give

$$F_A(q^2)+\frac{q^2}{m_\pi^2}F_P(q^2)+\frac{M_N^2-M_{N'}^2}{m_\pi^2}F_T(q^2) = \frac{a_\pi m_\pi^3}{(M_N M_{N'})^{1/2}}\frac{g_{N\pi N'}(q^2)}{(q^2+m_\pi^2)}. \quad (8)$$

As there is no evidence for the induced tensor term,[35] it may be neglected. Evaluating Eq. (8) at $q^2=0$ then gives the nuclear Goldberger-Treiman relation

$$g_{N\pi N'}(0)=\frac{(M_N M_{N'})^{1/2}}{a_\pi m_\pi}F_A(0). \quad (9)$$

Finally, the value of $g_{N\pi N'}(0)$ can be obtained from the $ft$ value for the $\beta$ decay of $N' \to N$,[36] since

$$|F_A(0)|^2=\frac{2\pi^3 \ln 2(2J_{N'}+1)}{3G^2\cos^2\theta_C m_e^5\{ft\}}, \quad (10)$$

where the weak interaction coupling constant $G=1.026\times10^{-5}/m_p^2$, the Cabibbo angle $\theta_C=0.257$, $m_e$ is the electron mass, and $J_{N'}$ is the spin of the nucleus $N'$.

A similar procedure can be applied to the nucleon $\beta$ decay. In this case, one obtains for nucleons that

$$g_A(q^2)+\frac{q^2}{m_\pi^2}g_P(q^2)=\frac{a_\pi m_\pi^3}{(m_n+m_p)}\frac{g_{p\pi n}(q^2)}{q^2+m_\pi^2}. \quad (11)$$

Evaluating this expression at $q^2=0$, one obtains a modified Goldberger-Treiman relation, namely

$$g_{p\pi n}(0)=\frac{(m_n+m_p)}{a_\pi m_\pi}g_A(0). \quad (12)$$

Here and in the following, the weak nucleon form factors have been denoted by $g_A$ and $g_P$, and the weak nuclear form factors have been denoted by $F_A$ and $F_P$. From the neutron $\beta$ decay,[37] we obtain $g_A(0)=1.239$,[38] and thus

$$g_{p\pi n}(0)=17.8. \quad (13)$$

From a dispersion theoretical analysis of pion-nucleon scattering, it is known that the physical coupling constant is[39]

$$g_{p\pi n}(-m_\pi^2)=19.3. \quad (14)$$

Thus, choosing a simple functional form for $g_{p\pi n}(q^2)$ expected to be valid for $-m_\pi^2 \le q^2 \le m_\pi^2$, we find that

$$g_{p\pi n}(q^2)=g_{p\pi n}(0)/[1+q^2/(4.92m_\pi)^2]^2. \quad (15)$$

The dependence of the nuclear vertex function $g_{N\pi N'}(q^2)$ could be determined from Eq. (8) if the two form factors, $F_A(q^2)$ and $F_P(q^2)$, were known. The pseudoscalar form factor may be estimated from the axial vector form factor. One has from the impulse approximation[13,40]

$$\frac{F_P(q^2)}{F_A(q^2)}=\frac{g_P(q^2)}{g_A(q^2)}. \quad (16)$$

With this expression for $F_P(q^2)$, it is then necessary to know only the ratio $g_P(q^2)/g_A(q^2)$ and $F_A(q^2)$. If the dependence on momentum transfer of $g_A(q^2)$ and $g_{p\pi n}(q^2)$ were identical, then we would obtain directly from (11)

$$\frac{g_P(q^2)}{g_A(q^2)}=\frac{-m_\pi^2}{m_\pi^2+q^2}. \quad (17)$$

However, from an analysis of neutrino scattering, Kim[33] finds

$$g_A(q^2)=g_A(0)/(1+q^2/45.8m_\pi^2)^2. \quad (18)$$

This difference increases the ratio of $g_P(q^2)/g_A(q^2)$ by a factor of 1.04.[41] For $|q^2| \le m_\pi^2$ this modification and corrections to the impulse approximation [Eq. (16)] are rather insignificant.[33]

The dependence on momentum transfer of the axial vector form factor may be obtained from the inelastic electron scattering form factor. In this approximation we first note that from the impulse approximation[15]

$$F_M(q^2)\cong\{F_M(q^2)\}_{\text{orbital}}+\{F_M(q^2)\}_{\text{spin}} \cong\{F_M(q^2)\}_{\text{orbital}}+\frac{g_V+g_M}{g_A}F_A(q^2), \quad (19)$$

where $F_M(q^2)$ is a weak magnetism nuclear form factor that contributes to the vector current in the decay $N' \to N+e+\nu$, and $(g_V+g_M)/g_A$ may be taken to be independent of momentum transfer $[=(1+3.7)/1.24]$. For nucleon transitions in which the initial and final states have no orbital angular momentum, which is approximately the situation for the cases of masses 6 and 12 considered here, the orbital contribution vanishes. Thus, Eq. (19) yields, for nuclei in which the spin contribution is dominant,

$$\frac{F_A(q^2)}{F_A(0)}\cong\frac{F_M(q^2)}{F_M(0)}. \quad (20)$$

Now the weak magnetism form factor can be related to the transverse inelastic electron scattering form factor $\mu(q^2)$ measured in the scattering to the analog state of $N'$. Using CVC[33] Kim shows that

$$\frac{F_M(q^2)}{F_M(0)} = \frac{\mu(q^2)}{\mu(0)} . \tag{21}$$

For $q^2 \lesssim m_\pi^2$ the inelastic electron scattering form factor can be fitted by the dipole form, from which Kim[33] obtains

$$\frac{F_A(q^2)}{F_A(0)} = \frac{1}{(1+q^2/M_N^2)^2} , \quad q^2 \lesssim m_\pi^2 \tag{22a}$$

where

$$M_N^2 = 2.0 m_\pi^2 \text{ for } {}^6\text{Li} \rightarrow {}^6\text{Be} \tag{22b}$$

and

$$M_N^2 = 2.6 m_\pi^2 \text{ for } {}^{12}\text{C} \rightarrow {}^{12}\text{N} . \tag{22c}$$

Now, taking Eqs. (8), (9), (16), (17), and (22), we obtain for $g_{N\pi N'}(q^2)$

$$\frac{g_{N\pi N'}(q^2)}{g_{N\pi N'}(0)} = \frac{1 - q^2/25m_\pi^2}{(1+q^2/M_A^2)^2} . \tag{23}$$

Without too much reflection one will recognize that the important assumption in this argument is that the nuclear vertex functions and the weak form factors all have dependence on momentum transfer similar to $\langle N' | \vec{\sigma}\tau\, e^{i\vec{q}\cdot\vec{x}} | N \rangle$.

Although the assumptions that were introduced to arrive at Eq. (23) are justified for $^6$Li and $^{12}$C, the justification is not so evident for $^{14}$N. The difficulty lies in the fact that although $^{14}$N is a $1^+$ nucleus, its total orbital angular momentum is dominantly $L=2$ (see Ref. 15). Thus, in Eq. (19) the orbital term $\{F_M(q^2)\}_{\text{orbital}}$ is not negligible. In fact, Goulard *et al.* take the extreme position that the spin contribution $\{F_M(q^2)\}_{\text{spin}}$ is negligible in obtaining the dependence of $g_{N\pi N'}(q^2)$ on momentum transfer. However, their analysis was intended for use at larger $q^2$ than we are considering since they assume that $\{F_M(0)\}_{\text{spin}} = 0$, which is probably not exact. With no other guide to the separation of $\{F_M(q^2)\}_{\text{spin}}$ and $\{F_M(q^2)\}_{\text{orbital}}$, we use Eq. (20) for $F_A$, along with the functional form of Goulard *et al.*[15] for $F_M(q^2)/F_M(0)$. We then obtain for mass 14

$$\frac{g_{N\pi N'}(q^2)}{g_{N\pi N'}(0)} = (1 - q^2/25m_\pi^2)(1 + q^2/m_\pi^2)\, e^{-0.38q^2/m_\pi^2} . \tag{24}$$

If we were to follow the argument of Goulard *et al.*, the factor $1+q^2/m_\pi^2$ would be changed to $q^2/m_\pi^2$, with the consequence that the $p + {}^{14}\text{N} \rightarrow n + {}^{14}\text{O}$ cross section would vanish in the forward direction.

It should be noted that Eqs. (8) and (11), from which the magnitude of the vertex functions at $q^2 = 0$ and their dependence on momentum transfer were obtained, were derived by neglecting the higher order terms in $\langle N' | \phi | N \rangle$ and $\langle n | \phi | p \rangle$. However, it is the case that for $p + N \rightarrow n + N'$ we also neglect higher order contributions. Thus, to the extent that higher order contributions are similar, the vertex function $g_{N\pi N'}(q^2)$, as derived, is actually an effective coupling for the initial nucleus changing to the final nucleus with a pion somehow being produced. Thus, the cross sections predicted with this vertex function should be more accurate than one might initially expect. If one were to attempt to determine from the $p + N \rightarrow n + N'$ data the physical coupling constant $g_{N\pi N'}(-m_\pi^2)$, then it would be necessary to understand the differences in the higher order contributions, both in the charge exchange reaction itself and the PCAC application.

### E. Results

The comparisons between the predicted and experimental cross sections at 0° are especially important since they are independent of the form factors. The momentum transfer is approximately zero, so that the magnitude of the cross section is determined solely by the values of $g_{p\pi n}(0)$ and $g_{N\pi N'}(0)$, which are obtained from PCAC. [See Eqs. (9) and (12).] In Table II the predicted values of $g_{N\pi N'}(0)$ and those extracted from the data are shown, while in Fig. 9, the predicted cross sections are displayed with the data.

The sensitivity of the theoretical predictions to variations in the ingredients of the calculation is shown in Fig. 10. It is clear that absorption is a significant, yet not an overwhelming, modification of the Born amplitudes. Furthermore, the traditional prescription for the absorption correction yields results that are only half as large as those obtained with our prescription, and they are much lower than the mass 6 and 12 data. Our treatment of distortions yields a reduction in the Born cross sections similar to that given by a traditional

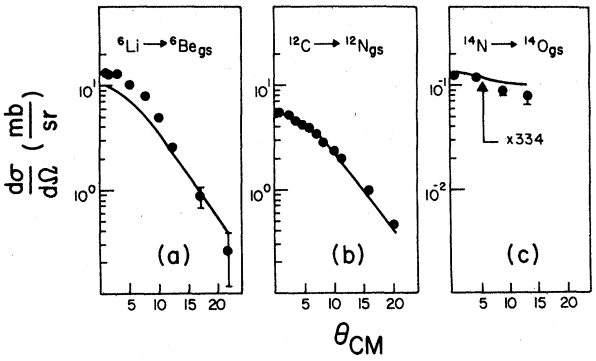


FIG. 9. Comparison of our distorted wave one-pion exchange calculation to the measured differential cross sections in the reaction (a) $p + {}^6\text{Li} \rightarrow n + {}^6\text{Be}$ (ground state), (b) $p + {}^{12}\text{C} \rightarrow n + {}^{12}\text{N}$ (ground state), and (c) $p + {}^{14}\text{N} \rightarrow n + {}^{14}\text{O}$ (ground state).

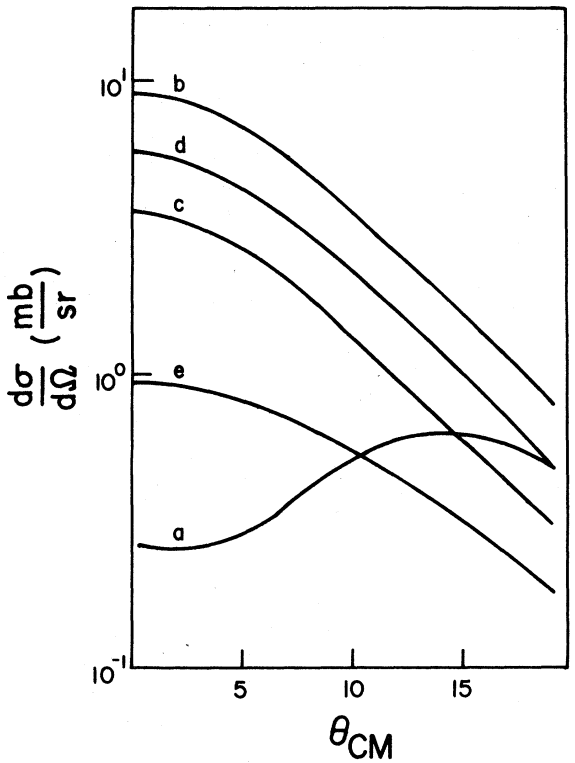


FIG. 10. Various calculations of the $^{12}C$ differential cross sections. Detailed descriptions of the calculations appear in the text. The curves represent: (a) Born approximation, including the extraordinary terms, (b) Born approximation, excluding the extraordinary terms, (c) DWBA, excluding the extraordinary terms, with the distortion modifications made with the $(S_i^j)^{1/2}T^j(S_f^j)^{1/2}$ prescription used in elementary particle physics (Refs. 7 and 8), and (d) DWBA, excluding the extraordinary terms, with the distortion modifications introduced by the authors. Curve (e) represents the $\theta$ or $q^2$ dependence of the form factor product

$$g_{p\pi n}(q^2)g_{N\pi N'}(q^2)/\{g_{p\pi n}(0)g_{N\pi N'}(0)\}.$$

DWIA calculation.[13] The validity of our approximation is discussed in the Appendix. The shapes of the cross sections are seen to be rapidly falling with angle; about one-half of this decline is due to the form factor, with the rest being due to the pion propagator. Finally, one sees that if the extraordinary terms are left in the Born amplitudes, then the results bear no resemblance to the data.

## IV. DISCUSSION AND CONCLUSIONS

As seen in Table II and Fig. 8, the agreement between the theory and experiment is fair for $^6Li$ and $^{12}C$. The 30% disagreement for $^6Li$ (15% is the amplitudes) could be largely due to the fact that $g_{N\pi N'}(0)$ was determined from the $F_A(0)$ value of the $^6He$ $\beta$ decay, since the $F_A(0)$ value for the unstable $^6Be$ is unknown. Other contributions to the discrepancy could come from the 7% normalization error, uncertainties in the $S$ matrix, and inadequacies of the absorption model. It is also possible that there are small contributions from interactions other than one-pion exchange. At any rate, the agreement that is achieved for $^6Li$ and $^{12}C$ is good evidence that these reactions are dominated by one-pion exchange.

The $^{14}N$ case is much different, however. Here, the measured cross sections are a factor of 100 lower than for $^6Li$, but they are still a factor of 300 larger than the values predicted from one-pion exchange and PCAC. This is not a failure of the model, however, as the model predicts one-pion exchange amplitudes, which in this case are expected to be extremely small. These amplitudes are so small, in fact, that other mechanisms which are normally small effects, such as two-step process and rho exchange, are no longer negligible. Thus, the model is predicting that

TABLE II. The initial nucleus ($N$), pion ($\pi$), final nucleus ($N'$) vertex function $g_{N\pi N'}(0)$ as calculated from nuclear $\beta$ decay, assuming the validity of the modified Goldberger-Treiman relation. It is compared to $g_{N\pi N'}(0)$ extracted from our 0.3° differential cross sections using our absorption modified one-pion exchange model, assuming one-pion exchange dominance.

| Target | $N' \rightarrow N$ $ft$ (sec) | {Ref.} | $g_{N\pi N'}(0)$ {PCAC} | $g_{N\pi N'}(0)$ {experiment} | $(d\sigma/d\Omega)/0°$ (mb/sr) |
|---|---|---|---|---|---|
| $n$ | $1.076\times10^3$ | {42} | 17.8 | | 13 [a] |
| $^6Li$ | $8.157\times10^2$ [b] | | 69.2 | 60.9 | 13.1 |
| $^{12}C$ | $1.315\times10^4$ | {44} | 59.5 | 59.9 | 5.56 |
| $^{14}N$ | $2.14\times10^7$ | {15} | 0.994 | 18.0 | 0.13 |

[a] Extrapolation of 152 MeV data from Ref. 43.

[b] The $^6He$ $ft$ value (Ref. 45) was actually used, since the value for the short lived $^6Be$ was not known.

these are the processes that will be measured. In that sense, the fact that the cross sections are so much smaller than the mass 6 and 12 cases is a success of the model. Since this case is a measurement of reactions such as two-step processes and rho exchange, it provides an estimate of the magnitude of such processes in light nuclei and indicates the limits of one-pion exchange dominance.

The inhibition of one-pion exchange in the $p + {}^{14}N_{g.s.} \rightarrow n + {}^{14}O_{g.s.}$ reaction is due to the structure of the two nuclei. The $^{14}N_{g.s.}$ nucleus is predominantly a $^3D_1$ state, whereas the $^{14}O_{g.s.}$ nucleus is a combination of $^1S_0$ and $^3P_0$ states.[15] The $^{14}O$ (7.77 MeV) state, however, is a $J^\pi = 2^+$ state, so it may be $^1D_2$. Such a state could be obtained from $^{14}N_{g.s.}$ by a spin-flip transition, so one would expect it to be dominated by one-pion exchange. Therefore, the similarity of the experimental differential cross sections for the $p + {}^{14}N \rightarrow n + {}^{14}O$ (7.77 MeV) transition to those for the mass 12 case suggests that it is dominated by one-pion exchange and that the 7.77 MeV state of $^{14}O$ is predominantly a $^1D_0$ state.

If the differential cross sections for $^6Li$ and $^{12}C$ were due exclusively to one-pion exchange, then they would provide a definitive test of the application of PCAC to nuclei. However, if the $^{14}N$ cross sections are interpreted as interactions other than one-pion exchange, which could also occur in the $^6Li$ and $^{12}C$ transitions, then the test is obscured. One can estimate the maximum effect that this background could have on the one-pion exchange amplitudes by assuming only one independent helicity amplitude for $^{14}N$ and that this amplitude interferes coherently with the primary amplitude of one-pion exchange at 0°. Using

$$\frac{d\sigma}{d\Omega} = \frac{1}{(2J_i + 1)} |f|^2 , \tag{25}$$

this gives $|f_{^6Li}(0)| = 6.27$, $|f_{^{12}C}(0)| = 2.36$, and $|f_{^{14}N}(0)| = 0.62$. Thus, the measured cross sections may deviate from those of one-pion exchange and, hence, those predicted by PCAC, by up to 20% for $^6Li$ and 50% for $^{12}C$. If the applicability of PCAC to nuclei is to be tested better than this with the data measured here, then the background contributions will actually have to be calculated.

Since PCAC predicts amplitudes, we have found it to be valid at the 25% level. Based on what one has learned about PCAC in particle physics, was this expected? Well, even if one firmly believes in the validity of PCAC when applied to elementary particles such as a pion, one could imagine various complications that could arise when it is applied to a compound system as a whole. The fact that these complications are so small is remarkable. Furthermore, there have so far been only two impressive tests of PCAC in the particle physics domain, other than the Goldgerger-Treiman relation for which PCAC was created to explain. These are the Adler consistency condition, which is a relation between the nuclear coupling constant and the pi-nucleon off-mass shell scattering amplitude,[46] and the Adler-Weisberger sum rule, which predicts the weak axial vector coupling constant in terms of off-mass shell pion-proton total cross sections.[47] Both relations are derived using PCAC, and they appear to be valid to 10% and 5%, respectively. The test that we have made lends further credence to PCAC.

Since PCAC seems to be valid for nuclei, what are its applications? Perhaps its most important use would be to help unravel the nuclear force. In most nuclear transitions, there are more pieces to the interaction than one-pion exchange, and it is a complex problem to disentangle and identify the pieces. However, for transitions in which the final state $\beta$ decay to the initial state is allowed and measurable, the pion contribution can be predicted from PCAC, thereby simplifying the problem.

In conclusion, we find that there are certain types of nuclear reactions in which the nucleus acts as a filter for the nuclear force, allowing only one-pion exchange and reactions which are usually a very small component of nucleon-nucleus scattering in the forward direction at intermediate energies. Of the three cases studied here, $^6Li$ and $^{12}C$ had large, sharply forward-peaked angular distributions, whereas that for $p + {}^{14}N \rightarrow n + {}^{14}O_{g.s.}$ was extremely small and gently forward peaked. One-pion exchange calculations were made by treating the nucleus as an elementary particle. When the initial nucleus-pion-final nucleus coupling constant was assigned the value predicted by PCAC, the results were in fair and good agreement with $^6Li$ and $^{12}C$, respectively, but they were a factor of 300 lower than the $^{14}N$ data. If the $^{14}N$ data are taken as a background level to one-pion exchange for $^6Li$ and $^{12}C$, then we have tested the applicability of PCAC to nuclei at the 25% level and found it to be valid.

## V. ACKNOWLEDGMENTS

It is a pleasure to acknowledge the assistance of Dr. C. C. Foster in the design and construction of the neutron beam line and shielding arrangements. The support of Professor R. E. Pollock and Professor G. T. Emery throughout this work has been appreciated. We would like to thank Professor K. Vasavada for his theoretical assistance during the proposal and analysis stage. Professor

H. Primakoff, Professor B. Goulard, and Professor F. Petrovich were kind enough to elucidate the problems in $^{14}$N. Finally, we thank Dr. H. Foeische of the BNL Accelerator Division for arranging the loan of the sweeping magnet, without which our experiment would not have been possible. This work was supported in part by the National Science Foundation and the Department of Energy.

## APPENDIX: DWBA IN MOMENTUM SPACE

The goal of this appendix is to find a method of modifying the Born amplitudes for inelastic scattering to account for the distortions of elastic scattering, without the need of complex calculations. It is hoped that the success of the absorption model in elementary particle physics means that this is possible, although we realize that the absorption model must be modified before it can be applied to a nucleus. The form we use for including distortions will be derived in the eikonal approximation, and the final form is by no means exact. Although the derivation will be done in coordinate space, the final result will be written in terms that are easily transposed to momentum space.

The general form of the scattering amplitude for scattering from a potential $V$ is given by[48]

$$T_{\beta\alpha} = \int u_\beta^*(\vec{r}) V(\vec{r}) \chi_\alpha^+(\vec{r}) d^3r \,, \tag{A1}$$

where $u_\beta$ is a plane wave representing the final state and $\chi_\alpha^+$ is the solution of the Schrödinger equation with potential $V$ representing the initial state. We wish to consider the case

$$V = V_1 + V_2 \,, \tag{A2}$$

where $V$ is the total nuclear potential and $V_2$ is the potential corresponding to the inelastic transition in question. We will make the DWBA approximation that the effect of $V_2$ on $\chi_\alpha^+$ can be ignored.

In the eikonal approximation, one writes[49]

$$\chi_\alpha^+(\vec{r}) = u_\alpha(\vec{r}) \exp -\frac{i}{v} \int_{-\infty}^{z} V_1(b, z') dz' \,, \tag{A3}$$

where $V$ has been taken as being spherically symmetric, $v$ is the velocity of the projectile, and cylindrical coordinates have been used. If one defines

$$E(b) = \left\langle \exp -\frac{i}{v} \int_{-\infty}^{z} V_1(b, z') dz' \right\rangle_{\text{Average over } z} \,, \tag{A4}$$

then Eqs. (A1) and (A3) give

$$\begin{aligned} T_{\beta\alpha} &= \int u_\beta^*(\vec{r}) [V_1(r) + V_2(r)] u_\alpha(\vec{r}) \left\{ \exp -\frac{i}{v} \int_{-\infty}^{z} V_1(b, z') dz' \right\} dz\, d^2b \\ &\simeq \int E(b) u_\beta^*(\vec{b}, z) [V_1(b, z) + V_2(b, z)] u_\alpha(\vec{b}, z) dz\, d^2b \,. \end{aligned} \tag{A5}$$

Since $V_1$ does not contribute to the inelastic scattering, and since it is of no longer range than $V$, it will not contribute to the last expression of Eq. (A5). (If $V$ were of longer range than $V_2$, then its effects would be seen after the inelastic scattering had occurred, so they would have to be dealt with. The absence of this effect is the major difference between our calculation and those of traditional nuclear physics and is a result of treating the nucleus as an elementary particle.) Thus, Eq. (A5) becomes

$$T_{\beta\alpha} = \int E(b) T_{\beta\alpha}^{\text{Born}}(\vec{b}) d^2b \,, \tag{A6}$$

where $T_{\beta\alpha}^{\text{Born}}(\vec{b})$ is the Born scattering amplitude defined by

$$T_{\beta\alpha}^{\text{Born}} = \int T_{\beta\alpha}^{\text{Born}}(\vec{b}) d^2b \,. \tag{A7}$$

It would be useful if $E(b)$ could be replaced by something simpler than (A4). Since the value of the integral over $V_1$ in Eq. (A4) for $z = 0$ is one-half of its value for $z = \infty$, it seems reasonable to use

$$E(b) \simeq D(b)^{1/2} \,, \tag{A8a}$$

$$D(b) \equiv \exp -\frac{i}{v} \int_{-\infty}^{\infty} V_1(b, z') dz' \,. \tag{A8b}$$

However, the integral in Eq. (A8b) can be identified as twice the elastic scattering phase shift for the angular momentum corresponding to the impact parameter $b$. This is seen by calculating the elastic scattering $S$ matrix from Eq. (A3), using Eq. (A8b):

$$\begin{aligned} \langle \beta | S | \alpha \rangle &= \int u_\beta^*(\vec{b}, z) \chi_\alpha^+(\vec{b}, z = \infty) dz\, d^2b \\ &= \int u_\alpha^*(\vec{b}, z) u_\alpha(\vec{b}, z) D(b) dz\, d^2b \\ &= \langle \beta | \alpha \rangle + \int u_\beta^*(\vec{b}, z) u_\alpha(\vec{b}, z) [D(b) - 1] dz\, d^2b \,. \end{aligned} \tag{A9}$$

Now, for small scattering angles,

$$(\vec{k}-\vec{k}')\cdot\vec{r} = kz - \vec{k}'\cdot\vec{r}$$
$$= kz - k'z\cos\theta - k'\sin\theta\hat{x}\cdot\vec{b}$$
$$\simeq (k-k')z - k'b\sin\theta\cos\phi\,, \qquad \text{(A10)}$$

and from Ref. 50,

$$J_0(l\cos\theta) \simeq P_l(\cos\theta)\,. \qquad \text{(A11)}$$

Equation (A9) then gives

$$\langle\beta|S-1|\alpha\rangle = 2\pi\delta(k-k')\int e^{-ik'b\sin\theta\cos\phi} \times [D(b)-1]b\,db\,d\phi$$
$$= 4\pi^2\delta(k-k')\int J_0(k'b\sin\theta)[D(b)-1]b\,db\,. \qquad \text{(A12)}$$

Letting $b \to l/k$ and $\int l \to \sum_l$, Eqs. (A11) and (A12) give

$$\langle\beta|S-1|\alpha\rangle = 4\pi^2\delta(k-k')\sum_l P_l(\cos\theta)[D(b)-1]l/k^2$$
$$\simeq \frac{2\pi^2\delta(k-k')}{k^2}\sum_l (2l+1)P_l(\cos\theta) \times [D(l/k)-1]\,. \qquad \text{(A13)}$$

Equation (A13), however, is the expression relating the $S$ matrix to the phase shifts if one takes $D(l/k) = e^{2i\delta_l} = S_l$.

Thus, transforming Eq. (A6) to angular momentum space and using Eq. (A8a), one has

$$T_{\beta\alpha} = \sum_l S_l^{1/2} T^{\text{Born}}_{\beta\alpha,l}\,. \qquad \text{(A14)}$$

Actually, the $S$ matrix depends on the total angular momentum $j$ as well. Furthermore, Eq. (A14) was derived assuming that the elastic scattering potential was the same before and after the inelastic reaction. Since this is not true for $(p,n)$ scattering, one must take an average of the two potentials. However, since the resultant $S$ matrices are very similar, the exact method of averaging is unimportant. Also, the Born amplitudes are easier to decompose in terms of $j$, whereas the $S$ matrices depend on $j$ and $l$. An exact calculation would decompose the $j$th partial wave into $l=j+\frac{1}{2}$ and $l=j-\frac{1}{2}$ components, but an unweighted average should be sufficient. Thus, we write the scattering amplitudes as

$$T_{\beta\alpha} = \sum_j S_j^{1/2} T^{\text{Born}}_{\beta\alpha,j}\,, \qquad \text{(A15a)}$$

$$S_j^{1/2} = \tfrac{1}{4}[S_i^{j,j+1/2})^{1/2} + (S_i^{j,j-1/2})^{1/2} + (S_f^{j,j+1/2})^{1/2} + (S_f^{j,j-1/2})^{1/2}]\,, \qquad \text{(A15b)}$$

where $S_i^{j,l}$ ($S_f^{j,l}$) is the elastic scattering matrix for the potential corresponding to the incident (outgoing) projectile.

In order to get an idea of how accurate Eq. (A8a) is, consider the case with the largest absorption, $l=0$. If Eq. (A4) is considered as an average of a sum of terms where $z$ ranges from $-R$ to $R$, and the terms are grouped into pairs of $\pm z$, then the largest deviation from the average would be expected to occur for the pair $z=\pm R$. For $z=-R$, the term is 1, and for $z=R$, the term is $S_l$. A typical value for $S_{1/2\,0}$ is $e^{-0.5+1.0i}$. Using this, one has

$$\tfrac{1}{2}(1+S_{1/2\,0}) = 0.664 + i0.255\,, \qquad \text{(A16a)}$$

$$(S_{1/2\,0})^{1/2} = 0.684 + i0.373\,. \qquad \text{(A16b)}$$

These terms differ in magnitude by about 13%. Since they represent the worst case of the worst case, the error in replacing (A4) by $\sqrt{S_l}$ may only incur an error of 5% or less.

It is not clear, however, how much error one makes in using the second relation in Eq. (A5). It should be a reasonable approximation if $V_1 R/v$ is not too large.

One would also expect to have to satisfy the conditions under which the eikonal approximation is valid,[51]

$$\frac{k^2}{2m} \gg \frac{|V(r)|}{4}\,, \quad |V(r)| \gg \frac{\lambda}{4\pi}\left|\frac{dV(r)}{dz}\right|\,. \qquad \text{(A17)}$$

For the cases considered here, this translates to

$$130\ \text{MeV} \gg 4.2\ \text{MeV}\,, \quad 17\ \text{MeV} \gg 1.4\ \text{MeV}\,, \qquad \text{(A18)}$$

so the eikonal approximation is a reasonable one.

---

*Present address: Indiana University Cyclotron Facility, Milo B. Sampson Lane, Bloomington, Indiana 47405.

†Present address: Department of Physics, University of Illinois, Champaign, Illinois 61820.

[1] A. Bohr and B. Mottelson, *Nuclear Structure* (Benjamin, New York, 1969), Vol. I.

[2] L. Durand and Y. T. Chiu, Phys. Rev. B 137, 1530 (1965).

[3] C. W. Kim and H. Primakoff, Phys. Rev. B 139, 1447 (1965).

[4] M. L. Goldberger and S. B. Treiman, Phys. Rev. 110, 1178 (1958).

[5] W. G. Love, A. Scott, F. T. Baker, W. P. Jones, and J. D. Wiggens, Phys. Lett. 73B, 277 (1978).

[6] A. Pickeleseimer and G. E. Walker, Phys. Rev. C 17,

237 (1978).
[7]K. Gottfried and J. D. Jackson, Nuovo Cimento 34, 735 (1964).
[8]L. Durand and Y. T. Chiu, Phys. Rev. B 139, 646 (1965).
[9]H. Hogaasen and J. Hogaasen, Nuovo Cimento 39, 941 (1965).
[10]J. R. Comfort, Proceedings from the Conference on $(p,n)$ Reactions and the Nucleon-Nucleon Force, Telluride, Colorado, 1979.
[11]R. Schaeffer, in *Two Body Force in Nuclei*, proceedings of the Gull Lake Conference on the two body force in nuclei, 1971, edited by S. M. Austin and G. Crawley (Plenum, New York, 1972).
[12]F. Petrovich, Nucl. Phys. A251, 143 (1975).
[13]R. M. Haybron and H. McManus, Phys. Rev. B 136, 1730 (1964).
[14]J. Delorme, Nucl. Phys. B19, 573 (1970).
[15]B. Goulard, B. Lorazo, H. Primakoff, and J. D. Vergados, Phys. C 16, 1999 (1977).
[16]M. Ericson and A. Figureau, Nucl. Phys. B3, 609 (1967).
[17]T. E. O. Ericson and M. P. Locher, Nucl. Phys. A148, 1 (1970).
[18]H. Toki and W. Weise, Phys. Rev. Lett. 42, 1034 (1979).
[19]O. N. Jarvis, C. Whitehead, and M. Shah, Nucl. Phys. A184, 615 (1974).
[20]P. T. Debevec, G. L. Moake, and P. A. Quin, Nucl. Inst. Methods 166, 467 (1979).
[21]D. F. Measday and J. N. Polmieri, Phys. Rev. 161, 1071 (1967).
[22]K. Erkelenz, Phys. Rev. 23, 191 (1974).
[23]P. K. Williams, Phys. Rev. 181, 1963 (1969).
[24]G. Breit and R. D. Horacz, in *High Energy Physics*, edited by E. H. S. Burhop (Academic, New York, 1967), Vol. I.
[25]G. E. Brown and A. D. Jackson, *The Nucleon-Nucleon Interaction* (North-Holland, Amsterdam, 1976).
[26]M. H. MacGregor, R. A. Arndt, and R. M. Wright, Phys. Rev. 182, 1714 (1969).
[27]G. F. Chew, Phys. Rev. 112, 1380 (1958).
[28]A. Ashmore, W. H. Range, R. T. Taylor, M. B. Townes, L. Castillejo, and R. F. Peierls, Nucl. Phys. 36, 258 (1962).
[29]P. Cziffra and M. F. Moravcsik, Phys. Rev. 116, 226 (1959).
[30]O. Dumbrajs, Ann. Phys. (N.Y.) 118, 249 (1979).
[31]G. L. Moake and P. T. Debevec, Phys. Rev. C 21, 25 (1980).
[32]P. Schwandt, Indiana University Cyclotron Facility Internal Report No. 77-8.
[33]C. W. Kim, Riv. Nuovo Cimento 4, 189 (1974).
[34]M. Gell-Mann and M. Levy, Nuovo Cimento 16, 705 (1960).
[35]H. Brandle, L. Grenacs, J. Lang, L. Ph. Roesch, V. L. Telegdi, P. Truttmann, A. Weiss, and A. Zehndev, Phys. Rev. Lett. 40, 306 (1978).
[36]G. L. Moake, Indiana University Cyclotron Facility Internal Report No. 79-2.
[37]C. J. Christensen, A. Nielsen, A. Bahnsen, W. K. Brown, and B. M. Rustad, Phys. Rev. D 5, 1628 (1972).
[38]R. J. Blin-Stoyle, *Fundamental Interactions and the Nucleus* (North-Holland, Amsterdam, 1973).
[39]M. L. Perl, *High Energy Hadron Physics* (Wiley, New York, 1974).
[40]Y-W. P. Hwang and H. Primakoff, Phys. Rev. C 16, 397 (1977).
[41]C. W. Kim and J. S. Townsend, Phys. Rev. D 11, 656 (1975).
[42]Reference 37; the $f$ function was calculated by J. N. Bahcall, Nucl. Phys. 75, 10 (1966).
[43]J. N. Palmieri and J. P. Wolfe, Phys. Rev. C 3, 144 (1971).
[44]R. E. McDonald, J. A. Becker, R. A. Chalmers, and D. H. Wilkinson, Phys. Rev. C 10, 333 (1974).
[45]D. H. Wilkinson and D. E. Alburger, Phys. Rev. C 10, 1993 (1974).
[46]S. L. Adler, Phys. Rev. B 137, 1022 (1965); 139, 1638 (1965).
[47]S. L. Adler, Phys. Rev. B 140, 736 (1965); W. I. Weisberger, Phys. Rev. 143, 1302 (1966).
[48]L. I. Schiff, *Quantum Mechanics* (McGraw-Hill, New York, 1968).
[49]See Ref. 39, p. 42.
[50]See Ref. 39, p. 60.
[51]See Ref. 39, p. 44.